Available online www.jocpr.com

Journal of Chemical and Pharmaceutical Research, 2015, 7(4):675-678

Research Article

ISSN : 0975-7384
CODEN(USA) : JCPRC5

Effect of Dy^{3+} substitution on the structural properties of barium hexaferrite nanoparticles

Varsha C. Chavan[1], Sagar E. Shirsath[2], Maheshkumar L. Mane[3*] and Surendra S. More[1]

[1]Department of Physics, Yashawantrao Chavan Mahavidyalaya, Tuljapur Dist. Osmanabad (MS), India
[2]Department of Physics, Vivekanand College, Aurangabad (MS), India
[3]Department of Physics, S. G. R. G. Shinde Mahavidyalaya, Paranda Dist. Osmanabad (MS), India

ABSTRACT

The present paper deals with the investigations on how the structural properties of M-type $BaFe_{12}O_{19}$ ferrite nanoparticles prepared by sol-gel auto-combustion technique depend on of Dy^{3+} substitution. X-ray diffraction study was carried out at room temperature reveals the formation of single Phase hexagonal structure. The XRD results were used to calculate lattice constant, X-ray density, porosity and strong influence of Dy^{3+} substitution

Keywords: M-type, X-ray diffraction, Nanoparticles

INTRODUCTION

Hexagonal ferrites fall in the category of hard magnetic materials. Now a day, hard ferrites pervade almost every sphere of modern technology. Hard ferrites play heavy role in electronic industry, electronic information industry, car industry, motor cycle industry etc, mean while, they are also widely used in medical treatment, mining and metallurgy, industrial automation, oil industry and civil industry [1]. In the hexaferrite family, M-type ferrite $BaFe_{12}O_{19}$ has attracted a lot of attention because of its excellent magnetic properties [2]. In recent years, scientific interest in the investigation of nanoscale M-type barium hexaferrite (BHF) has increased [3-6]. This interest is caused by a combination of unique magnetic properties of BHF, and its chemical and thermal stability [7, 8]. Nanoscale hexagonal ferrites are promising materials for the production of new generation of permanent magnets [9], high-density data recording and storage systems [10], various up-to-date microwave devices [11], etc.

The rare earth ions can be divided into two categories; one with the radius closes to Fe ions; while the other with ionic radius larger than Fe ions. The rare earth ions have unpaired 4f electrons and the strong spin orbit coupling of the angular momentum. Moreover, 4f shell of rare earth ions is shielded by $5S^25P^6$ and almost not affected by the potential field of surrounding ions. The interest in the area of rare earth substitution in the M-type hexaferrites has grown significantly over the past years as these materials have enhanced coercivity. Kool et al. [12] and Yamamoto [13] and substituted La and La–Co at barium site in $BaFe_{12}O_{19}$, respectively, and reported a significant increase in coercivity without a drop in remanence.

In the present work, the sol–gel auto-combustion method has been used for the fabrication of barium hexaferrites. The effect of Dy^{3+} substitution on the structural properties of barium hexaferrite has been discussed.

EXPERIMENTAL SECTION

Dysprosium (Dy) doped M-type barium hexaferrite nanoparticles with the generic formula $BaDy_xFe_{12-x}O_{19}$ ($x = 0.0$, 0.050 and 0.100) were prepared by sol-gel auto-combustion technique using AR grade nitrates of respective cations $Ba(NO_3)_2 \cdot 6H_2O$, $Dy(NO_3)_3 \cdot 6H_2O$, $Fe(NO_3)_3 \cdot 9H_2O$. Citric acid was used as chelating agent. All starting materials

were dissolved in de-ionized water with required molarities. The metal nitrate to citric acid ratio was mentioned at 1:3. The solutions of the precursors were mixed and heated on hot plate with violent stirring. The pH of the solution plays a major role in the formation of a compound. The pH of the solution was kept at 8 by using ammonia solution. The detail of synthesis technique was discussed in the literature reports [14-16]. X-ray diffraction patterns (XRD) were obtained using Philips X-ray diffractometer (Model PW 3710) with Cu-K_α radiations (λ = 1.5405 Å).

RESULTS AND DISCUSSION

In order to confirm the phase formation of $BaDy_xFe_{12-x}O_{19}$ (x = 0.0 0.050 and 0.100) hexaferrite nanoparticles the standard power X-ray diffraction technique in the region of 2θ = 20–80 with a step scan of 0.02°/min on a Philips diffractometer (Model PW1710) using Cu-Kα radiation (λ=1.5406 Å) is carried out at room temperature. The X-ray diffraction pattern for pure hexaferrite samples is shown in Figure 1. All the diffractions peaks matches well with single phase hexagonal ferrite with JCPDS file no 43-0002.

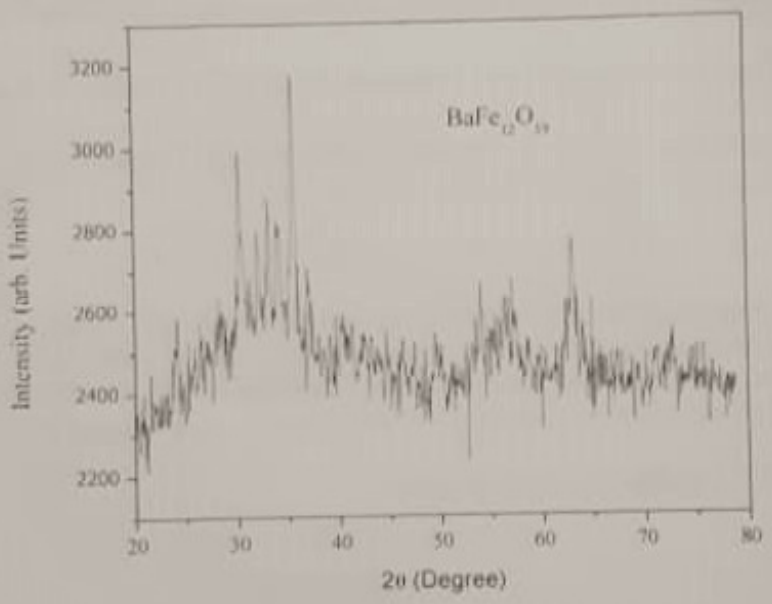

Figure 1: X-ray diffraction pattern for $BaDy_xFe_{12-x}O_{19}$ (x = 0.0) nanoparticles

It is observed from Figure 1 that the increase in the Dy^{3+} content causes the change in the intensity of the XRD characteristic peaks of $BaDy_xFe_{12-x}O_{19}$. Lattice parameters 'a' and 'c', as shown in Table 1, are calculated from the XRD data using equation [16]

$$\frac{1}{d^2} = \frac{4}{3}\left(\frac{h^2 + hk + k^2}{a^2}\right) + \frac{l^2}{c^2} \qquad (1)$$

where 'h, k, l' are Miller indices and 'd' is the inter-planer spacing. The value for the lattice parameters 'a' and 'c' increases regularly with the addition of Dy ion whereas there is a little or no variation in the d-spacing values with respect to the 2-theta values. The observed phenomenon can be justified on the basis that the ionic radii of dysprosium (1.04 Å) is comparatively higher than the ionic radius of Fe^{3+} (0.64 Å).

Table 1: Values of Lattice constant 'a' and 'c', c/a ration, cell volume 'V', particle size 'D', x-ray density 'd_x', bulk density 'd_b' and porosity '%P' for $BaDy_xFe_{12-x}O_{19}$

Comp. X	a (Å)	c (Å)	c/a	V $(Å)^3$	d_x (g/cm^3)	d_b (g/cm^3)	%P	D (nm)
0.0	5.889	23.67	4.019	710.906	5.192	3.64	29.90	34.45
0.050	5.889	23.98	4.072	720.216	5.155	3.78	26.67	45.64
0.100	5.892	24.11	4.0920	724.859	5.141	3.95	23.17	51.31

The volume of unit cell 'V' can be calculated from formula and values are tabulated in Table 1

$$V = \frac{\sqrt{3}}{2} a^2 c \quad (2)$$

The data reported in Table 1 indicates that cell volume V increases as Dy^{3+} cation concentration increases.

The crystallite size 'D' can be measured by the Scherer equation [17] which is expressed as

$$D = \frac{0.9\lambda}{\beta \cos\theta} \quad (3)$$

where 'λ' is wave length, 'β' is FWHM and 'θ' is the Bragg angle. The values of measured crystalline size were reported in the Table 1. The crystallite size is found to be in the range of 34.45 to 51.31 nm.

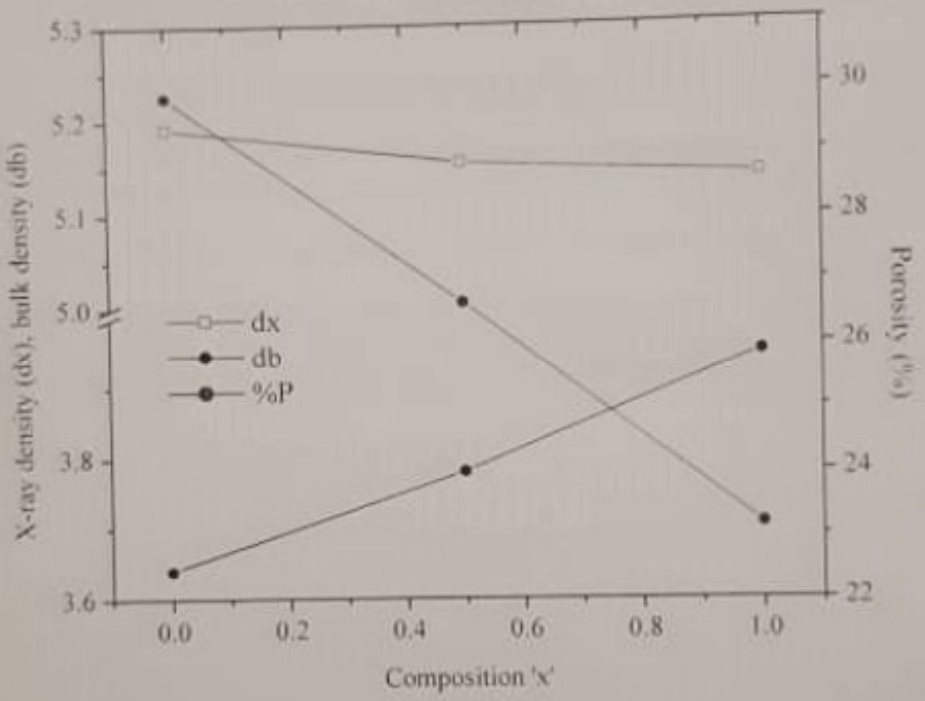

Figure 2: Variation of X-ray density, bulk density and porosity for $BaDy_xFe_{12-x}O_{19}$ (x = 0.00, 0.050 and 0.100) ferrite nanoparticles

X-ray density (theoretical density) 'd_x' is calculated by the formula

$$d_x = \frac{2M}{N_A V} \quad (4)$$

where, numeric factor denotes the number of formula units in a unit cell, 'M' is the molar mass, 'N_A' is the Avogadro's number and 'V' is the unit cell volume. The X-ray density is directly related to molecular weight and varies inversely with cell volume (V) which is again directly proportional to lattice parameter c. The bulk density (d_b) and porosity (%P) was also calculated [18] and values are presented in Table 1. The variation of X-ray density, bulk density and porosity with Dy^{3+} ion content is depicted in Figure 2.

CONCLUSION

Nanoparticels $BaDy_xFe_{12-x}O_{19}$ has been successfully synthesized by sol-gel auto-combustion technique. It is observed that the increase in the Dy^{3+} content causes the change in the intensity of the XRD characteristic peaks of $BaDy_xFe_{12-x}O_{19}$ (x = 0.0, 0.050 and 0.100). Lattice constant 'a' and 'c' increased with the increase in Dy^{3+} substitution. Dy^{3+} substitution also affects the other structural parameters such as density and porosity of BaM nanoparticles.

REFERENCES

[1] R. Grossinger, J. C. Tellez-Blanco, F. Kools, A. Morel, P. Tanaud, in: proceedings of the 8th International Conference on Ferrites, Kyoto, Japan, **2000**, 428, 18-21 September.
[2] A. Xia, D. Du, P. Li, Y. Sun, *J. Mater. Sci: Materials in Electronics*, **2011**, 22, 223-227
[3] T. Ugur, O. Husnu, G. T. Kevser, *J. Alloys Compds*, **2006,** 422 276-278
[4] M. Vérité, M. Valetas, A. Bessaudou, F. Cosset, J.C. Vareille, *J. Europ. Ceram. Society*, **2006,** 25 1689
[5] Nazmun Nahar Shams, Xiaoxi Liu, Mitsunori Matsumoto, Akimitsu Morisako, *J. Magn. Magn. Mater.*, **2005**, 290–291, 138-140
[6] L. Junliang, Z. Wei, G. Cuijing, Z. Yanwei, *J. Alloys Compds*, **2009** 479, 863-869
[7] H. Kojima, E. P. Wohl-farth (Eds.), North-Holland, Amsterdam, **1982**
[8] Y. A. Smit, H. P. Wijn, Ferrites: physical properties of ferrimagnetic oxides in relation to their technical application, Wiley-Inter Science, NewYork, **1959**
[9] S. P. Gubin, Y. U. A. Koksharov, G. B. Khomutov, G. Y. U. Yurkov, *Russian Chemical Reviews*, **2005**, 74, 489-520.
[10] F. Lei, L. Xiagang, Y. I. Zhang, V. P. Dravid, C. A. Mipkin, *Nano Letters*, **2003,** 3, 757-760.
[11] Sergey V. Lebedev, Carl E. Patton, Michael A. Wittenauer, Laxmikant V. Saraf and Ramamoorthy Ramesh, *Journal of Applied Physics*, **2002**, 91, 4426.
[15] F. Kools, A. Morel, M. Rossignol, O. Isnard, R. Grossinger, J.M.L. Breton, P. Tenaud, *J. Magn. Magn. Mater.*, **2002**, 242-245, 1270-1276
[13] H. Yamamoto, M. Nagakura, and H. Terada, *IEEE Transactions on Magnetics*, **1990**, 26, 1144-1148
[14] Sagar E. Shirsath, Mahesh L. Mane, Yukiko Yasukawa, Xiaoxi Liu, Akimitsu Morisakoa, *Phys. Chem. Chem. Phys.*, **2014,** 16, 2347-2357
[15] B. G. Toksha, Sagar E. Shirsath, M. L. Mane, S. M. Patange, S. S. Jadhav, K. M. Jadhav, *J. Phys. Chem. C*, **2011,** 115, 20905-20912
[16] Vinod N. Dhage, M. L. Mane, A.P. Keche, C.T. Birajdar, K.M. Jadhav, *Physica B*, **2011**, 406, 789-793
[17] V.V. Awati, S.M. Rathod, Sagar E. Shirsath, Maheshkumar L. Mane, *J. Alloys Compds*, **2013**, 553, 157-162
[18] Vinod N. Dhage, M.L. Mane, M.K. Babrekar, C.M. Kale, K.M. Jadhav, *J. Alloys Compds*, **2011**, 509, 4394-4398